RESEARCH ARTICLE

Can nerve regeneration on an artificial nerve conduit be enhanced by ethanol-induced cervical sympathetic ganglion block?

Yoshiki Shionoya[1]*, Katsuhisa Sunada[2], Keiji Shigeno[3], Akira Nakada[3], Michitaka Honda[3], Tatsuo Nakamura[3]

1 Department of Dental Anesthesia, Nippon Dental University Hospital at Tokyo, Japan, **2** Department of Dental Anesthesiology, Nippon Dental University School of Life Dentistry at Tokyo, Tokyo, Japan, **3** Department of Bioartificial Organs, Institute for Frontier Medical Science, Kyoto University, Kyoto, Japan

* ysk.shionoya@gmail.com

Abstract

This study aimed to determine whether nerve regeneration by means of an artificial nerve conduit is promoted by ethanol-induced cervical sympathetic ganglion block (CSGB) in a canine model. This study involved two experiments—in part I, the authors examined the effect of CSGB by ethanol injection on long-term blood flow to the orofacial region; part II involved evaluation of the effect of CSGB by ethanol injection on inferior alveolar nerve (IAN) repair using polyglycolic acid-collagen tubes. In part I, seven Beagles were administered left CSGB by injection of 99.5% ethanol under direct visualization by means of thoracotomy, and changes in oral mucosal blood flow in the mental region and nasal skin temperature were evaluated. The increase in blood flow on the left side lasted for 7 weeks, while the increase in average skin temperature lasted 10 weeks on the left side and 3 weeks on the right. In part II, fourteen Beagles were each implanted with a polyglycolic acid-collagen tube across a 10-mm gap in the left IAN. A week after surgery, seven of these dogs were administered CSGB by injection of ethanol. Electrophysiological findings at 3 months after surgery revealed significantly higher sensory nerve conduction velocity and recovery index (ratio of left and right IAN peak amplitudes) after nerve regeneration in the reconstruction+CSGB group than in the reconstruction-only group. Myelinated axons in the reconstruction+CSGB group were greater in diameter than those in the reconstruction-only group. Administration of CSGB with ethanol resulted in improved nerve regeneration in some IAN defects. However, CSGB has several physiological effects, one of which could possibly be the long-term increase in adjacent blood flow.

Introduction

Functionally adequate recovery from peripheral nerve injury continues to be a clinical challenge. Recently, a bioabsorbable polyglycolic acid tube filled with collagen sponge (PGA-C) was developed [1], which has been confirmed to aid the regeneration of peripheral nerves in

our experimental and clinical trials [2–6]. Blood supply to the surrounding tissue is a critical factor in nerve regeneration using PGA-C tubes [6]. In case of nerve regeneration with PGA-C tubes, success or failure is affected by blood flow in the area of reconstruction; therefore, increase in long-term blood flow to the area of nerve reconstruction through PGA-C tubes might promote nerve regeneration.

Stellate ganglion block (SGB), a type of sympathetic blockade, has several physiological effects, one of which is increased blood flow to regional tissues in the head, face, and neck, depending on its sympatholytic effects [7–9]. Previous studies have used ethanol for achieving cervical sympathetic ganglion block (CSGB) instead of SGB [10, 11]. Therefore, CSGB with ethanol might result in a long-term increase in blood flow to the region innervated by the inferior alveolar nerve (IAN). Accordingly, the objective of part I of this study was to develop a canine SGB model employing ethanol to achieve CSGB. The objective of part II was to perform electrophysiological and histological assessment of the rate of regeneration of the IAN in our canine SGB model following excision and reconstruction of the nerve using a PGA-C tube.

Materials and methods

Part 1: Development of the canine CSGB by ethanol

Surgical procedure and measurement of nasal skin temperature and oral mucosal blood flow in the mental region.   These experiments employed seven male Beagles, each weighing 9.0–13.0 kg. Skin temperature was measured by infrared thermography (Neo Thermo TVS-700, NEC Avio, Tokyo, Japan; resolution, 320×240 pixels; thermal sensitivity, 0.08˚C). Before measurement, the dogs were acclimated for 30 min in a room at 25˚C. The distance between the infrared camera and the nose was 50 cm. Mean skin temperature was calculated from the thermogram using the Easy Thermo Analyzer software (Bitstrong, Tokyo, Japan). The average temperatures on the right and left sides served as baseline values.

Following thermography, the dogs were anesthetized with ketamine hydrochloride (5 mg/kg) and xylazine (1 mg/kg) and intubated. On the basis of the method of Terakawa et al. [9], mucosal blood flow was measured by laser Doppler flowmetry. The animals were placed prone, and mechanical ventilation was commenced with 1.5% sevoflurane in oxygen to achieve a stable end-tidal carbon dioxide pressure of 35 mmHg for 30 min. After hemodynamic and respiratory stabilization, left oral mucosal blood flow was measured for 1 min by laser Doppler flowmetry (ALF21, Advance, Tokyo, Japan). The flowmeter probe was fixed in position with a stent made from dental resin in order to minimize contact pressure and enable measurement at the same location each time. Blood flow was recorded continuously using the PowerLab 30 Data Acquisition System (ADInstruments, Bella Vista, Australia).

Three days after baseline measurement, left CSGB was administered under ketamine hydrochloride, xylazine, and sevoflurane anesthesia. The cervical sympathetic ganglion was exposed by left lateral thoracotomy at the second intercostal space, and 0.2 mL of 99.5% ethanol was injected using a 30-gauge needle under direct visualization (Fig 1). Starting from a week after CSGB, skin temperature and oral mucosal blood flow were measured once per week for 3 months. Blood flow values were recorded as percentage change from baseline. The antibiotic isepamicin sulfate (100 mg/day) was administered for a week after surgery.

Histological changes in canine cervical sympathetic ganglion following ethanol block. The seven dogs were euthanized 6 months after left CSGB. The left and right cervical sympathetic ganglia were removed, fixed in 10% neutral formalin, embedded in paraffin, sectioned, and stained with hematoxylin–eosin.

Fig 1. Left-side cervical sympathetic ganglion after injection of 99.5% ethanol.

Part 2: Development and assessment of the canine model of IAN reconstruction

Fabrication of the nerve conduit. An artificial nerve conduit composed of an absorbable PGA tube filled with an atelocollagen scaffold was fabricated using a tubular braiding machine equipped with 48 spindles, which carried 5 PGA fibers comprising bundles of 26 filaments. The surface of the polyglycolic acid (PGA) tube was exposed to plasma discharge to render it hydrophilic. It was then coated with amorphous collagen layers by repeated dipping into a 1% collagen hydrochloride solution, followed by drying. This coating process was repeated 10 times. The inner space of this collagen-coated tube was then filled with a collagen sponge. All collagen used in this study was atelocollagen extracted from young porcine skin by enzyme treatment (Nippon Meatpackers, Ibaraki, Japan) and tested for viruses. This particular atelo-collagen mainly consists of type I collagen (70–80%), with the remainder mainly being type III collagen. The antigenicity of the atelocollagen was minimal because of the removal of antigenic telopeptides of collagen molecules during enzymatic extraction. To control the rate of bioabsorption, the PGA-C tubes were subjected to dehydrothermal treatment (140°C; 24 h) in vacuo, which resulted in the crosslinking of collagen molecules. The final length of the tube was 14 mm, with the inner diameter and wall thickness being 3–4 mm and 5.0×10^{-5} m, respectively (Fig 2A and 2B). Before surgery, the tube was sterilized using ethylene oxide and cut in accordance with demand in the operating room.

Surgical procedure for the reconstruction-only group. The mandibles of seven male Beagles were exposed by a 5-cm transverse incision in the left mandibular gingiva under general anesthesia with ketamine hydrochloride, xylazine, oxygen, and sevoflurane. The proximal aspect of the mandible was then ground into a 3-cm × 8-mm rectangle through the posterior mental foramen, using a carbide dental bur. The left IAN was exposed by carefully removing the frontal part of the mandibular bone plate (dimensions, 3-cm × 8-mm; Fig 3A). The site corresponding to the root apex of the first molar was established as the reconstruction site. The IAN was then transected with a scalpel, and a 10-mm segment was removed. The proximal and distal stumps of the severed nerve were both inserted into the nerve tube to a depth of 2
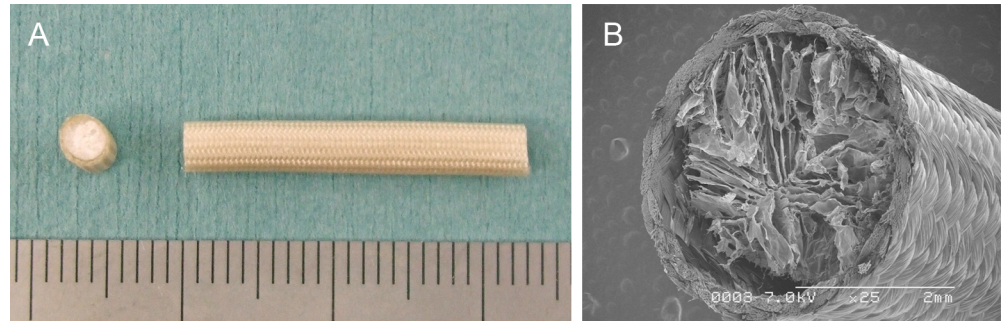
Fig 2. Gross image (A) and scanning electron micrograph (B) of a polyglycolic acid tube filled with collagen sponge.

mm. The tube was then sutured to the proximal and distal nerve ends with 8–0 epineural nylon sutures with the aid of a surgical microscope (Fig 3B), and the bone plate was replaced in its original site in the mandible; the wound was then closed. The implanted PGA–collagen tube was 14 mm in length and 2 mm in diameter. The antibiotic isepamicin sulfate (100 mg/day) was administered for a week after surgery.

Surgical procedure for the reconstruction+CSGB group. Seven male Beagles were subjected to IAN reconstruction with CSGB. Surgery was performed using the same techniques as those employed in the reconstruction only group. A week after reconstruction, left CSGB was administered with 99.5% ethanol according to the thoracotomy technique described in Part 1.

Electrophysiological study. Three months after reconstruction, sensory nerve action potential (SNAP) and sensory nerve conduction velocity (SCV) of the IAN were measured on both sides using the Neuropack Σ orthodromic recorder (Nihon Kohden, Tokyo, Japan). Sensory nerve action potential was determined by the average response amplitude at 10 kHz
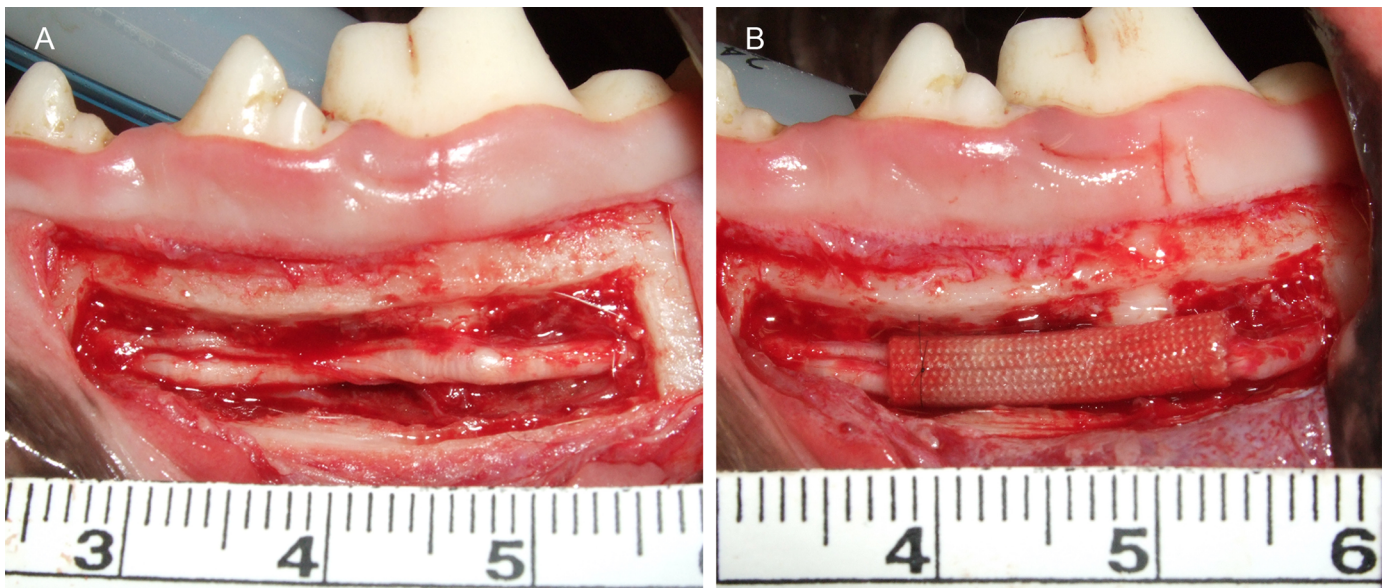

Fig 3. (A) Pre-reconstruction image of the left inferior alveolar nerve (IAN) exposed by removal of bone. (B) Post-reconstruction image of the left IAN reconstructed using a polyglycolic acid–collagen tube.

upon 20 applications of electrical stimulation. Because the dogs had to be immobilized during measurement, ketamine hydrochloride (15 mg/kg) and xylazine (7 mg/kg) were injected intramuscularly, and a heating pad was used to maintain the body temperature at 37˚C. Latency was measured between stimulation and peak amplitude, with amplitude being defined as the period from the peak of the first phase to the trough of the second phase. These results were used to calculate the SCV and recovery index (peak amplitude of the left IAN of the reconstruction-only or reconstruction+CSGB group / peak amplitude of the right IAN of the reconstruction-only group) [12, 13].

Histological and morphological evaluation. After measurement of SCV and recovery index, the left IAN was harvested, including 1 cm of the nerve on both sides of the reconstructed site, in both treatment groups. The right IAN of the reconstruction-only group was harvested at the site corresponding to the harvest site on the left side. Harvested nerves were immersion-fixed in 2.5% glutaraldehyde in a 0.1 M cacodylate buffer solution (pH 7.4) at 48˚C for 24 h. Further, postfixation was performed with 2% osmium tetroxide solution at 48˚C for 4 h and potassium ferrocyanide/0.1 M phosphate buffer solution (pH 7.4) for 2 h. The nerve specimens were then dehydrated in a graded ethanol series and embedded in epoxy resin. The specimens were then cross-sectioned (0.5–1.0 μm) and stained with toluidine blue.

Using a light microscope (BZ-9000, Keyence, Osaka, Japan), the specimens were imaged at 400x magnification at the following positions along the nerves: left IAN—the center of the regenerated segment and 2 mm distal from the stump in both treatment groups; right IAN— the center of the IAN segment corresponding to the harvest site on the left side in the reconstruction-only group. Microscopy images of regions showing myelinated nerve fibers were selected. In each of these selected images, eight to ten areas of 100- × 100-μm^2 dimensions were established in a random and non-biased manner and evaluated for myelinated nerve fiber diameter (μm) and density (count / 100 × 100 μm^2), nerve tissue percentage (%), and G-ratio (myelinated axon diameter / myelinated nerve fiber diameter), using a commercially available software (Dynamic cell count, Keyence, Osaka, Japan). Data evaluation was performed in a non-blinded manner.

The epoxy resin-embedded specimens prepared for immunohistochemical analysis were observed by transmission electron microscopy (TEM; Hitachi H-7000, Hitachi High Technologies, Tokyo, Japan). Cross sections (thickness, 70–90 × 10^{-6} m) were prepared using an ultramicrotome and stained with Reynold's lead citrate and uranyl acetate.

Immunohistochemistry. Nerve sections at the same sites as those described above were stained with anti- neurofilament and anti-S100 antibodies. Following immersion fixation in 2.5% glutaraldehyde in a 0.1 M cacodylate buffer solution (pH 7.4) at 48˚C for 24 h, the nerve specimens were embedded in paraffin according to the routine procedure. For primary antibodies, mouse anti-human neurofilament protein monoclonal antibody (N1591, Dako Japan, Kyoto, Japan) was incubated with polyclonal rabbit anti-S100 antibody (Z0311, Dako Japan, Kyoto, Japan). After washing with phosphate-buffered saline, the secondary antibody was labeled with horseradish-peroxidase and incubated for 30 min. The stained cross sections (0.5–1.0 μm) were observed under a light microscope.

Statistical analysis

Skin temperature, myelinated nerve fiber diameter and density, G-ratio, and SCV were compared using Dunnett's test. Oral mucosal blood flow and nerve tissue percentage were compared using Steel's test. Recovery index was compared using unpaired t-test. The level of statistical significance was set at 5% (P < 0.05; Kyplot, KyensLab, Tokyo, Japan).

Ethics statement

This study was conducted in accordance with the Guiding Principles in the Care and Use of Animals and approved by the Committee for Animal Research of Kyoto University (Kyoto, Japan; authorization numbers: R-16-16). All sections of this report adhere to the ARRIVE (Animal Research: Reporting of In Vivo Experiments) guidelines. Mice, rats, and rabbits have a short life expectancy and small body size. Therefore, it is not possible to perform precise surgical procedures in these animals. For this reason, we thought it necessary to use dogs. Experiments on nerve regeneration conducted using PGA-C tubes have so far used beagle dogs [1, 6]. Male beagles were purchased from SNBL, Ltd (Kagoshima, Japan) and housed at the Institute for Frontier Medical Science, Kyoto University, under controlled kennel conditions (12-h light:dark cycle). In accordance with standard care procedures, the dogs were housed in separate cages and provided solid food and water ad libitum. The veterinary staff monitored the animals on a daily basis. Intravenous fluids were used in the care of animals during all surgical procedures. Electrocardiographic readings, heart rate, and oxygen saturation were recorded during surgery. During thoracotomy, 1% lidocaine was used as a local anesthetic. Since analgesics could have influenced the experimental results, their necessity was evaluated when there were any signs of pain or distress. However, because there were no findings reminiscent of pain after surgery, analgesics were not used. In accordance with the regulations of the Committee for Animal Research, Kyoto University, a humane endpoint, such as euthanasia at an appropriate time, was to be considered for animals that experienced severe pain. At the end of the study, all dogs were euthanized by intravenous administration of an overdose of pentobarbital sodium, and all efforts were made to minimize suffering.

Results

Part 1: Development of the canine CSGB by ethanol

A week after CSGB, nasal skin temperature and average oral mucosal blood flow on the left side had increased by $8.8 \pm 1.1°C$ and $51 \pm 12\%$, respectively, in comparison with the baseline values (Fig 4A and 4B). While the increase in average skin temperature lasted 10 weeks on the
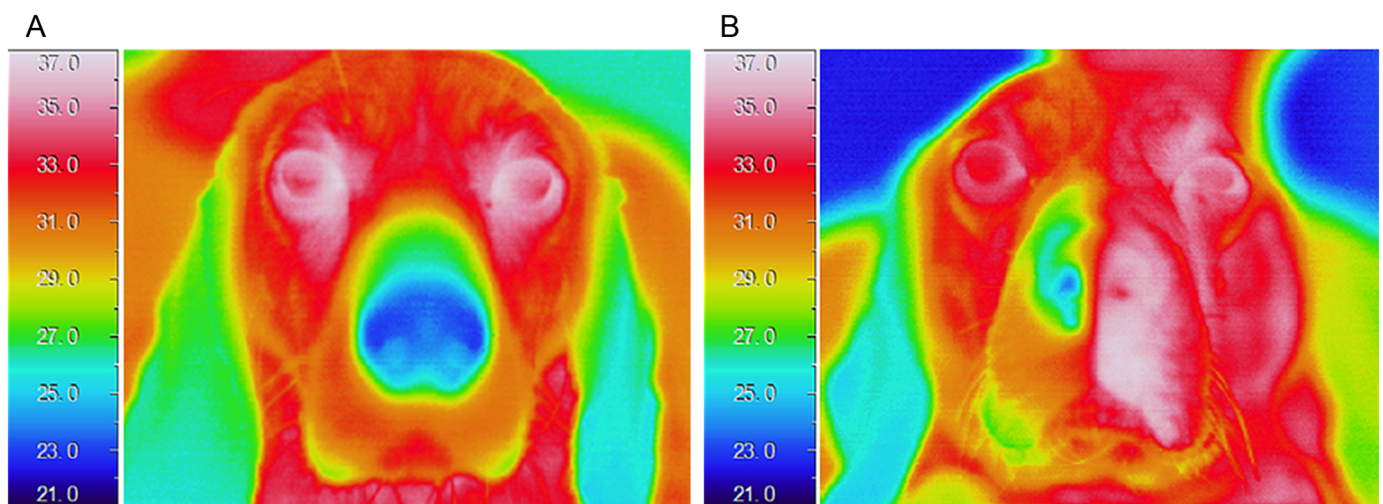

Fig 4. (A) Thermogram acquired before left cervical sympathetic ganglion block (CSGB) by ethanol injection. There was no difference in bilateral skin temperature. (B) A week after left CSGB, skin temperature on the left side was significantly higher compared to the baseline value.
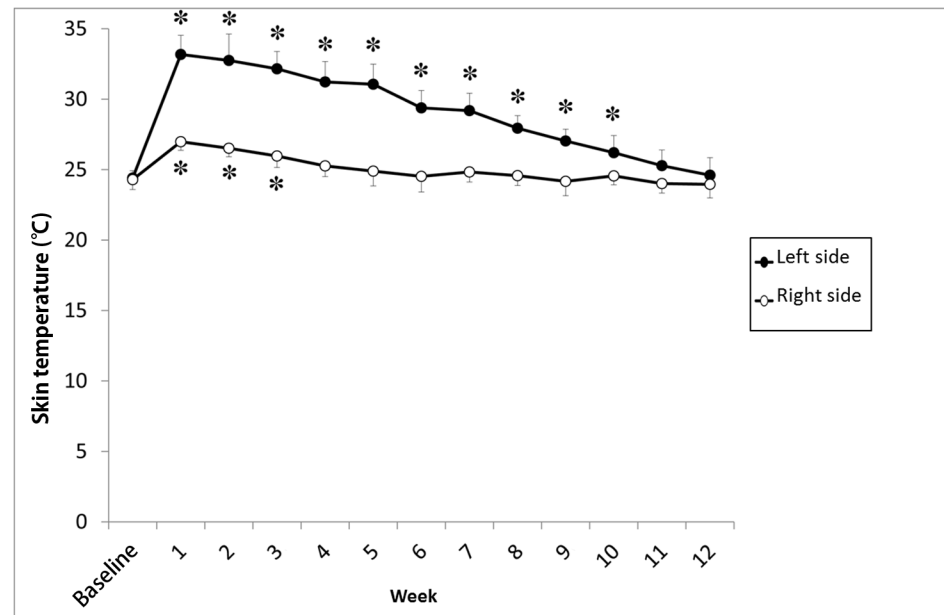
https://doi.org/10.1371/journal.pone.0189297.g004

Fig 5. Changes in average nasal skin temperature after left cervical sympathetic ganglion block (CSGB). There was a significant increase in average nasal skin temperature after CSGB, which lasted for 10 weeks on the left side and 3 weeks on the right side. Values are expressed as mean ± SD. *P < 0.01 in comparison with the baseline value.

left side and 3 weeks on the right side (Fig 5), the increase in blood flow on the left side lasted for 7 weeks (Fig 6).

While histological sections of the left cervical sympathetic ganglia exhibited no viable ganglion cells 6 months after ethanol injection (Fig 7A), those of the right side exhibited ganglion cells throughout the cervical sympathetic ganglia (Fig 7B).

Part 2: Development and evaluation of the canine model of IAN reconstruction

Electrophysiological study. All dogs that underwent IAN reconstruction with and without CSGB were evaluated for SNAP, the results of which are summarized in Table 1. The recovery index and SCV in the reconstruction+CSGB group were significantly greater than those in the reconstruction-only group.

Gross view and histological and morphological evaluation. At 3 months post-reconstruction, PGA-C tubes at the reconstruction site were absorbed, and the nerve, covered by fibrous tissue, exhibited regeneration (Fig 8A and 8B). There were no differences in gross findings between the reconstruction-only and reconstruction+CSGB groups.

Toluidine blue staining. Large numbers of myelinated nerve fibers were observed at the central and distal segments of the regenerated IAN in the reconstruction-only and reconstruction+CSGB groups (Fig 9A and 9B). Images of the normal control (central segment of the right IAN in the reconstruction-only group) are presented in Fig 9C.

The results of morphological evaluation are summarized in Table 2. Myelinated nerve fiber diameters and densities and nerve tissue percentages at both the central and distal segments of the regenerated left IAN in the reconstruction+CSGB group were significantly greater than those in the reconstruction-only group. The G-ratios at both the central and distal segments of
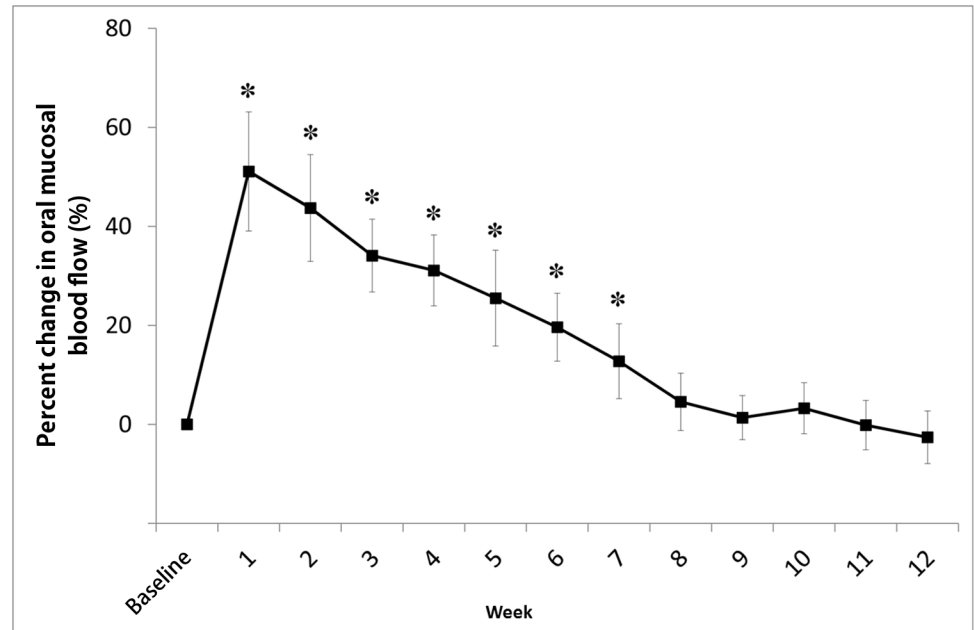
Fig 6. Percent changes in oral mucosal blood flow in the left mental region after cervical sympathetic ganglion block (CSGB). Blood flow was measured in the region dominated by the left mental arterial branch. The proportion of oral mucosal blood flow on the left side after CSGB remained significantly higher than that at baseline for up to 7 weeks. Values are expressed as mean ± standard deviation; *$P < 0.01$ in comparison with the baseline value.

https://doi.org/10.1371/journal.pone.0189297.g006

the regenerated left IAN in the reconstruction+CSGB group were significantly lower than those in the reconstruction-only group.

TEM. Nerve specimens of both treatment groups exhibited myelinated and unmyelinated nerve fibers and Schwann cells (Fig 9D and 9E). The reconstruction+CSGB group exhibited
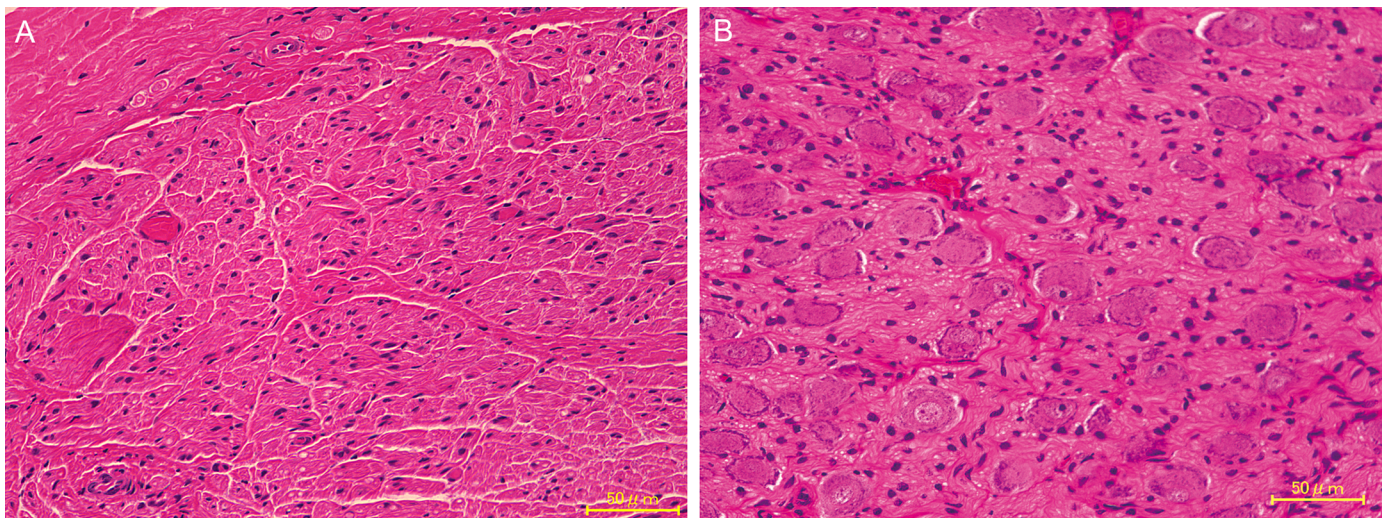

Fig 7. Light microscopy images of hematoxylin–eosin-stained transverse sections of the left (A) and right (B) cervical sympathetic ganglia at 6 months after ethanol injection. While the left side exhibited no ganglion cells in the entire ganglion, the right side exhibited ganglion cells throughout the ganglion. Scale bars, 50 μm.

https://doi.org/10.1371/journal.pone.0189297.g007

Table 1. Electrophysiological findings in the IAN at 3 months after surgery.

	Sensory nerve conduction (m/s)	Recovery index
Normal control	48.5 ± 2.8	—
Reconstruction-only group	36.8 ± 2.9*	0.22 ± 0.04
Reconstruction+CSGB group	42.0 ± 2.4*,#	0.35 ± 0.06#

Data are presented as mean ± standard deviation (n = 7). IAN, inferior alveolar nerve; CSBG, cervical sympathetic ganglion block.

*P < 0.05 in comparison with normal control;

#P < 0.05 in comparison with the reconstruction-only group

Normal control: central segment of the right IAN in the reconstruction-only group; Recovery index: peak amplitude of the left IAN of the reconstruction-only or reconstruction+CSGB group / peak amplitude of the normal control

https://doi.org/10.1371/journal.pone.0189297.t001

greater myelin sheath thickness than the reconstruction-only group. Images of the normal control are presented in Fig 8F.

Immunohistochemical staining. Nerve specimens of both the reconstruction-only and reconstruction+CSGB groups showed NF-stained axons and S100-positive Schwann cells at the central and distal segments of the regenerated left IAN (Fig 10).

Discussion

This is the first report to describe the successful promotion of nerve regeneration on an artificial nerve conduit by ethanol-induced CSGB. In comparison with the reconstruction-only group, the reconstruction+CSGB group exhibited significantly greater SCV and recovery index, which suggests that reconstruction with CSGB promoted IAN regeneration in the PGA-C tube. Myelinated nerve fiber count and diameter and myelin sheath thickness are the most reliable parameters for assessment of nerve regeneration. In addition, SNAP has been reported to be correlated with nerve fiber diameter and myelin sheath thickness [14, 15]. In regenerated nerves, the myelin sheath matures and thickens as the axon reaches the end of the distal segment [16]; thus, the relatively small G-ratio of the reconstruction+CSGB group demonstrates the progression of myelinated nerve regeneration.
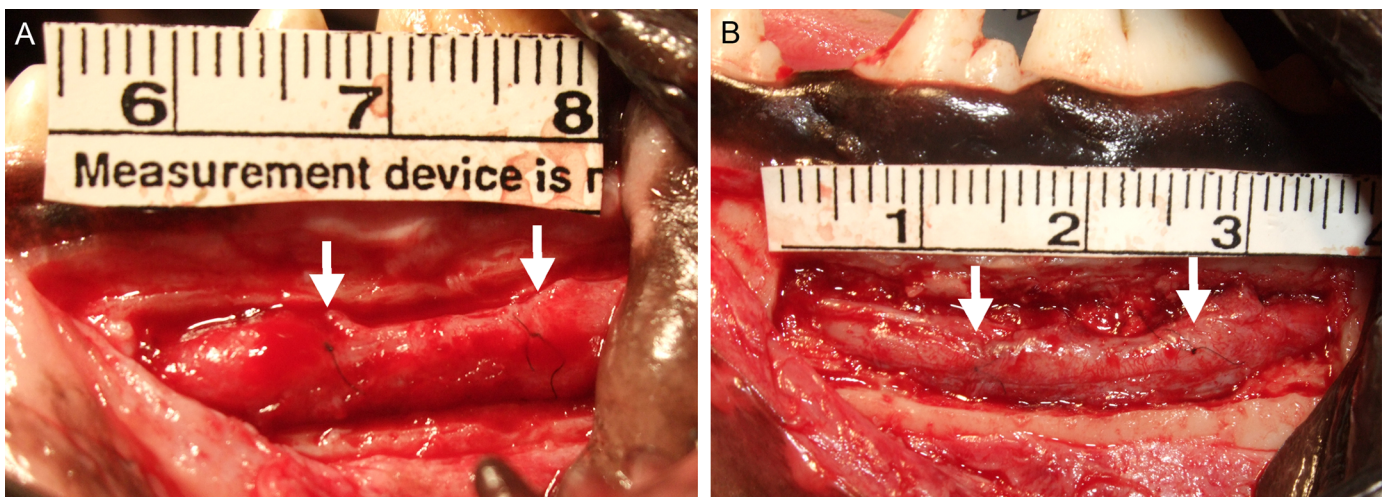

Fig 8. Gross images of regenerated inferior alveolar nerve in the reconstruction (A) and cervical sympathetic ganglion block (B) groups. Nerve regeneration (region between white arrowheads) was observed in both groups.

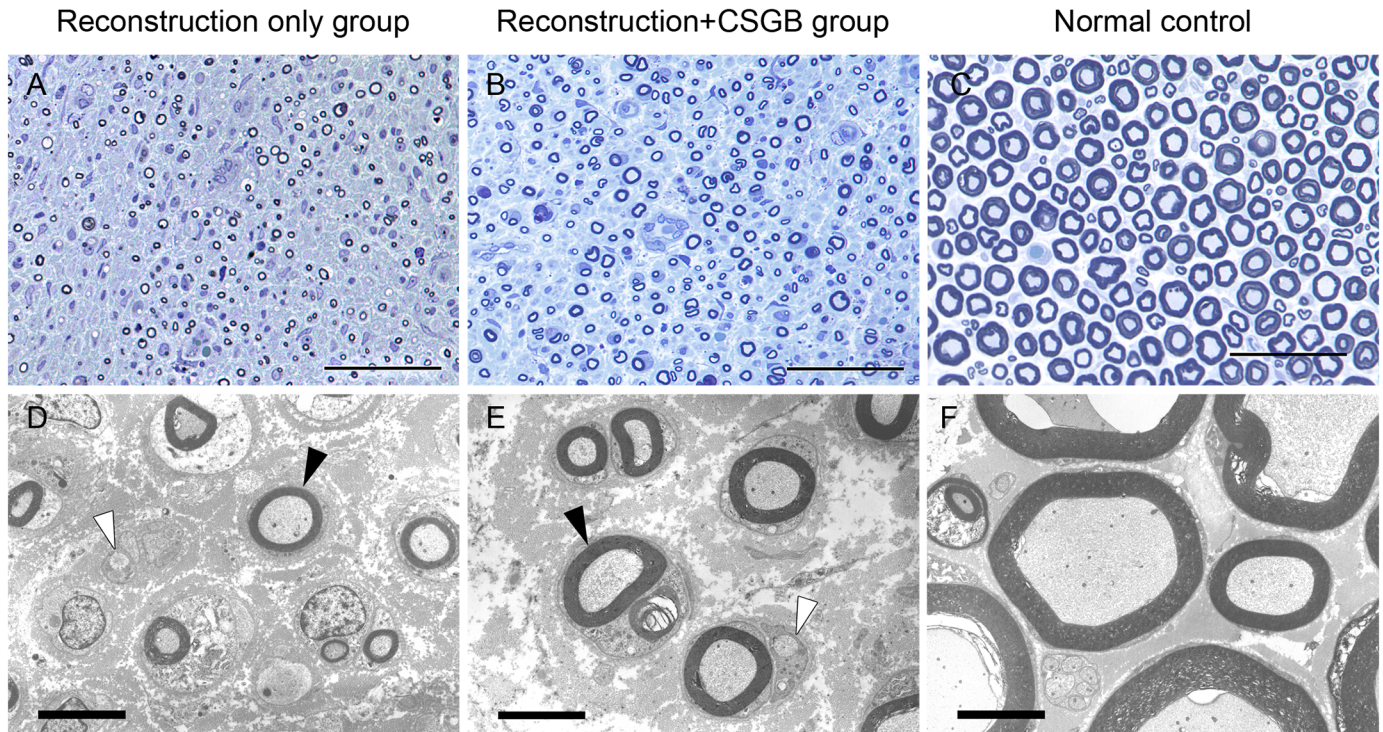https://doi.org/10.1371/journal.pone.0189297.g008

Fig 9. Semi-thin transverse sections (A–C; toluidine blue staining) and transmission electron microscopy images (D–F) of the regenerated inferior alveolar nerve (IAN) at 3 months post-reconstruction. Distal segments of the regenerated left IAN in the reconstruction-only (A, D) and reconstruction + cervical sympathetic ganglion block (reconstruction+CSGB; B, E) groups. (C, F) Central segment of the right IAN in the reconstruction-only group (normal control). Black and white arrowheads indicate myelinated and non-myelinated nerve fibers, respectively. Scale bars, 50 µm (A–C) and 5 µm (D–F).

When a nerve gap is so long that end-to-end tension-free suturing becomes difficult, it is necessary to employ another method for bridging the gap to allow the fibers to cross over and reach the distal nerve stump. The most widely used technique in this scenario is autologous nerve grafting. The use of autologous nerve grafts has yielded successful results in many studies [17–19], although it also has certain disadvantages such as the need for a second surgical procedure, possibility of loss of donor nerve function, limited supply of donor nerves, and

Table 2. Morphological findings in the IAN at 3 months after surgery.

		Myelinated nerve fiber diameter (µm)	Myelinated nerve fiber density (count/100 µm²)	Proportion of nerve tissue (%)	G ratio
Normal control		8.83 ± 3.11	103 ± 8	41.3 ± 3.9	0.62 ± 0.03
Reconstruction-only group	Center	4.27 ± 1.5*	126 ± 20*	11.6 ± 2.1*	0.75 ± 0.04*
	Distal	3.47 ± 1.21*	109 ± 17*	7.3 ± 2.0*	0.74 ± 0.04*
Reconstruction+CSGB group	Center	5.11 ± 1.98*#	140 ± 22*#	15.9 ± 3.0*#	0.68 ± 0.05*#
	Distal	4.53 ± 1.36*$	123 ± 15*$	12.5 ± 2.1*$	0.69 ± 0.04*$

Data are presented as mean ± standard deviation (n = 7). IAN, inferior alveolar nerve; CSGB, cervical sympathetic ganglion block.

*$P < 0.05$ in comparison with normal control;

#$P < 0.05$ in comparison with the central segment of the left IAN of the reconstruction-only group;

$$P < 0.05$ in comparison with the distal end of the left IAN of the reconstruction-only group;

Normal control: central segment of the right IAN in the reconstruction-only group; G ratio: myelinated axon diameter / total myelinated fiber diameter

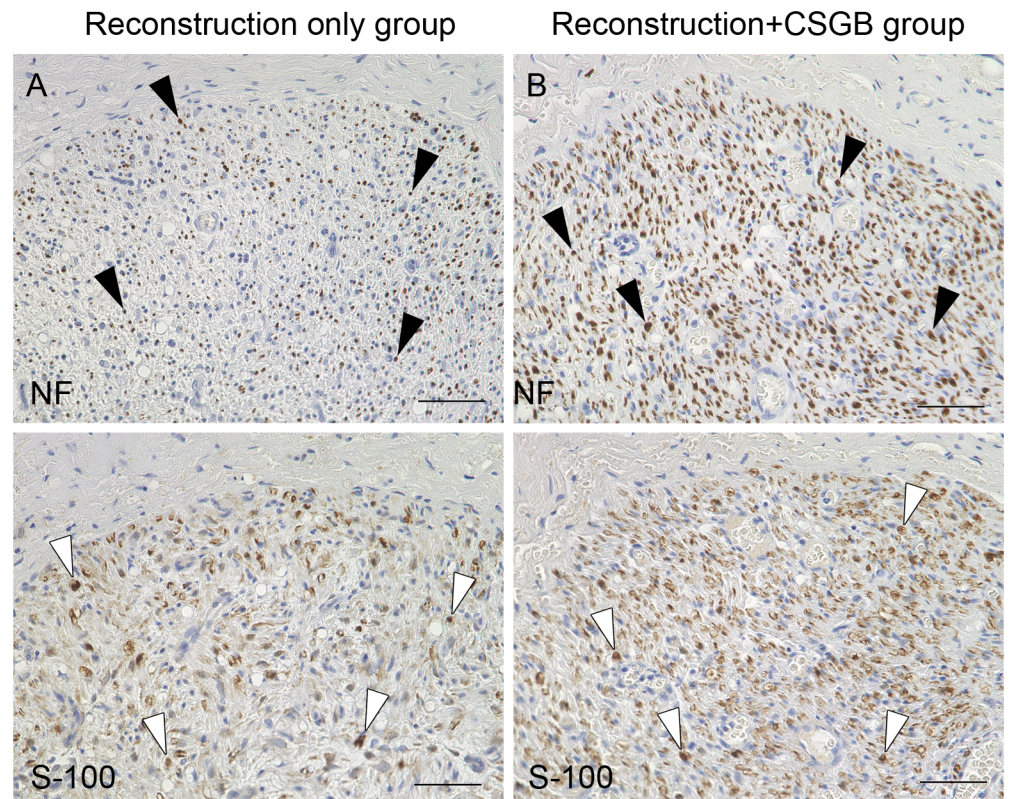Reconstruction only group   Reconstruction+CSGB group

Fig 10. Immunohistochemistry images of distal segments of the regenerated left inferior alveolar nerve at 3 months post-reconstruction (neurofilament and S100 staining). (A, C) reconstruction-only group; (B, D) reconstruction + cervical sympathetic ganglion block (CSGB) group. Black arrowheads indicate regenerated axons. White arrowheads indicate Schwann cells. Scale bars, 50 μm.

https://doi.org/10.1371/journal.pone.0189297.g010

dimensional mismatch between the impaired nerve and the graft [20–22]. In addition, because donor nerves are routinely obtained from a purely cutaneous source in order to minimize the resulting deficit, repaired motor axons must, by necessity, grow under less than favorable conditions [23, 24]. These disadvantages have led to the development of several alternative techniques, such as those involving the use of artificial nerve guides [25, 26].

Nakamura et al. [1] developed a PGA-collagen tube that uses a collagen scaffold as the support structure (PGA-C tube) and demonstrated that the tube allowed regeneration across a short gap of approximately 15 mm, with significantly higher levels of reinnervation than that obtained using autografts in a canine nerve-defect model. This PGA-c tube has been in clinical use since 2002 for human patients with peripheral nerve injuries and has provided some promising results [2–5].

In our study, we conducted electrophysiological, histological, and morphological evaluation at 3 months post-reconstruction. As described in our previous report [1], at 8 weeks after reconstruction of peroneal nerve deficits of 15-mm length using PGA-C tubes, most of the PGA fibers had been absorbed, and the axons ran through the structure in the proximal-to-distal direction. In a pilot study, which we conducted with reference to our previous report, when a 10-mm defect of the IAN was reconstructed with PGA-C tubes, the PGA fibers were absorbed within 3 months after surgery. Although regeneration was not yet complete at 3 months after reconstruction, it was confirmed that the axons ran through the structure in the proximal-to-distal direction. The present study focused on whether regeneration is promoted

by CSGB induced by ethanol injection and not on whether regeneration is completed. There-fore, we believe that it was necessary to perform comparisons during the regeneration stage. For these reasons, we decided on the 3-month time point for electrophysiological evaluation.

Peripheral nerve regeneration requires adequate blood flow. de la Torre and Goldsmith [27] reported that transposition of the omentum increases blood flow and promotes spinal nerve fiber growth. Oxygen supply is a particularly important factor in nerve regeneration; hyperbaric oxygen treatment has been reported to promote sciatic nerve regeneration in rats [28]. The use of artificial tubes in nerve regeneration helps localize Schwann cells, which regu-late the secretion of neurotrophic factors—including nerve growth factor, brain-derived neu-rotrophic factor, and neurotrophin-3 [29–31]—which have been reported to be beneficial for regeneration [32, 33]. In the present study, the result of S100 immunostaining revealed the presence of Schwann cells in the regenerated segment in the reconstruction+CSGB group. This result suggests that the CSGB-induced increase in blood flow aided nerve regeneration by increasing oxygen supply to the regenerated segment and, thereby, enhancing aerobic metabo-lism, resulting in increased ATP production and Schwann cell activity and promoting the pro-duction of neurotrophic factors. Increased blood flow has also been suggested to suppress edema at the nerve repair site and produce a favorable environment for nerve regeneration. However, CSGB has not only the effect of increasing blood flow but also other physiological effects, such as production of many types of cytokines [34, 35]. In this study, we only focused on the effect of CSGB on increasing blood flow; however, other physiological effects might have influenced the promotion of nerve regeneration. In this regard, we believe that further research is needed in the future.

In the present study, CSGB by ethanol resulted in increased blood flow in the mental arte-rial branch and facial artery. At 6 months after CSGB, no neurons were observed in the cervical sympathetic ganglion, which, we believe, indicates that ethanol-induced CSGB provides reli-able long-term blockade of the cervical sympathetic ganglion. However, the increases in blood flow and skin temperature demonstrated by our SGB models were not permanent. Alborch et al. [36] reported that, while goats exhibited increased cerebral blood flow following removal of the superior cervical sympathetic ganglion, the proportion of blood flow returned to pre-surgical levels 15–25 days after the procedure. One conceivable reason for this phenomenon is that increase in blood flow results in vasodilation and collateral circulation, causing blood flow to shift to the contralateral side. Nasal thermography findings in the present study revealed increased skin temperature on the contralateral side as well, which indicated that increase in blood flow on the side of nerve block resulted in increased blood flow on the contralateral side through anastomosis of the left and right facial arteries.

In this study, we chose ethanol to achieve assured sympathetic ganglion block for experi-mental purposes. However, in clinical practice, neurolysis of the stellate ganglion poses the risk of development of permanent Horner's syndrome (ptosis and miosis) [37]. In nerve regenera-tion, in order to achieve effective blood-flow increase by SGB with a local anesthetic, it is thought that several administrations of SGB are necessary. The conventionally used blind tech-nique for SGB can cause various adverse effects, including epidural, subarachnoid, and intra-vascular injection, hematoma formation, and esophageal injury [38, 39]. However, in recent times, the use of ultrasound guidance has made it possible to reduce the adverse effects of SGB [40]. Noninvasive SGB administered using physical modalities such as linearly polarized near-infrared irradiation can be clinically used as an alternative to conventional invasive SGB [41, 42]. Whether noninvasive SGB using linearly polarized near infrared light is effective for increasing local blood flow requires further research; however, we believe that it holds poten-tial as an alternative procedure.

In both treatment groups, the findings of TEM revealed several different stages of myelin sheath formation, suggesting incomplete regeneration. Moreover, the absolute values of SCV and SNAP of the regenerated IAN were lower than those of the normal control (central segment of the right IAN in the reconstruction-only group), which might have been because of the regeneration still being in progress.

The present findings could contribute to advances in surgical techniques, leading to improved outcomes of treatment for traumatic injury-induced trigeminal neuropathy using nerve guide tubes. Future studies should focus on the potential efficacy of SGB in facilitating repair at the cellular level.

This study has some limitations. We established the SGB model for an IAN injury that was completely encircled by bone. This creates a specific situation of blood flow from the three remaining sides, which is not typically seen in most cases of peripheral nerve injury. Further studies would be necessary to validate the present results in a more traditional nerve injury model. In addition, to prevent ethanol-induced damage to surrounding tissues, nerve blockade by surgical sympathectomy may be considered.

Conclusion

Cervical sympathetic ganglion block via ethanol injection increases blood flow in the region supplied by the mental branch of the IAN. In the reconstruction+CSGB group, this increase in blood flow might have promoted nerve regeneration after reconstruction using a PGA-C tube.

Supporting information

S1 File. ARRIVE guidelines checklist.
(PDF)

Acknowledgments

Author Contributions

Conceptualization: Yoshiki Shionoya, Katsuhisa Sunada, Keiji Shigeno, Tatsuo Nakamura.

Data curation: Yoshiki Shionoya, Katsuhisa Sunada, Keiji Shigeno, Akira Nakada, Michitaka Honda, Tatsuo Nakamura.

Formal analysis: Yoshiki Shionoya, Katsuhisa Sunada.

Funding acquisition: Katsuhisa Sunada, Tatsuo Nakamura.

Investigation: Yoshiki Shionoya, Keiji Shigeno, Akira Nakada, Michitaka Honda, Tatsuo Nakamura.

Methodology: Yoshiki Shionoya, Katsuhisa Sunada, Keiji Shigeno, Tatsuo Nakamura.

Project administration: Katsuhisa Sunada, Keiji Shigeno, Tatsuo Nakamura.

Resources: Keiji Shigeno, Akira Nakada, Michitaka Honda.

Software: Yoshiki Shionoya.

Supervision: Katsuhisa Sunada, Tatsuo Nakamura.

Validation: Yoshiki Shionoya, Keiji Shigeno, Akira Nakada, Michitaka Honda.

Visualization: Yoshiki Shionoya, Keiji Shigeno.

Writing – original draft: Yoshiki Shionoya.

Writing – review & editing: Yoshiki Shionoya, Katsuhisa Sunada, Tatsuo Nakamura.

References

1. Nakamura T, Inada Y, Fukuda S, Yoshitani M, Nakada A, Itoi S, et al. Experimental study on the regeneration of peripheral nerve gaps through a polyglycolic acid-collagen (PGA-collagen) tube. Brain Res. 2004; 1027(1–2): 18–29. https://doi.org/10.1016/j.brainres.2004.08.040 PMID: 15494153

2. Inada Y, Morimoto S, Moroi K, Endo K, Nakamura T. Surgical relief of causalgia with an artificial nerve guide tube: Successful surgical treatment of causalgia (Complex Regional Pain Syndrome Type II) by in situ tissue engineering with a polyglycolic acid-collagen tube. Pain. 2005; 117(3): 251–258. https://doi.org/10.1016/j.pain.2005.05.033 PMID: 16153773

3. Inada Y, Hosoi H, Yamashita A, Morimoto S, Tatsumi H, Notazawa S, et al. Regeneration of peripheral motor nerve gaps with a polyglycolic acid-collagen tube: technical case report. Neurosurgery. 2007; 61(5): E1105–E1107; discussion E1107. https://doi.org/10.1227/01.neu.0000303210.45983.97 PMID: 18091262

4. Yamanaka T, Hosoi H, Murai T, Kobayashi T, Inada Y, Nakamura T. Regeneration of the nerves in the aerial cavity with an artificial nerve conduit—reconstruction of chorda tympani nerve gaps. PLoS One. 2014; 9(4): e92258. https://doi.org/10.1371/journal.pone.0092258 PMID: 24691095

5. Seo K, Terumitsu M, Inada Y, Nakamura T, Shigeno K, Tanaka Y. Prognosis after surgical treatment of trigeminal neuropathy with a PGA-c tube: report of 10 cases. Pain Med. 2016; 17(12): 2360–2368. https://doi.org/10.1093/pm/pnw088 PMID: 28025370

6. Yoshitani M, Fukuda S, Itoi SI, Morino S, Tao H, Nakada A, et al. Experimental repair of phrenic nerve using a polyglycolic acid and collagen tube. J Thorac Cardiovasc Surg. 2007; 133(3): 726–732. https://doi.org/10.1016/j.jtcvs.2006.08.089 PMID: 17320572

7. Kakuyama M, Toda H, Osawa M, Fukuda K. The bilateral effect of stellate ganglion block on the facial skin blood flow. Reg Anesth Pain Med. 2000; 25(4): 389–392. https://doi.org/10.1053/rapm.2000.6450 PMID: 10925936

8. Kakuyama M, Toda H, Osawa M, Fukuda K. The bilateral effect of stellate ganglion block on the facial skin blood flow. Reg Anesth Pain Med. 2000; 25(4): 389–392. https://doi.org/10.1053/rapm.2000.6450 PMID: 10925936

9. Terakawa Y, Ichinohe T, Kaneko Y. Redistribution of tissue blood flow after stellate ganglion block in the rabbit. Reg Anesth Pain Med. 2009; 34(6): 553–556. PMID: 19916209

10. Ohno K, Oshita S. Transdiscal lumbar sympathetic block: a new technique for a chemical sympathectomy. Anesth Analg. 1997; 85(6): 1312–1316. PMID: 9390600

11. Wang YC, Wei SH, Sun MH, Lin CW. A new mode of percutaneous upper thoracic phenol sympathicolysis: report of 50 cases. Neurosurgery. 2001; 49(3): 628–634; discussion 634–626. PMID: 11523673

12. Suzuki Y, Tanihara M, Ohnishi K, Suzuki K, Endo K, Nishimura Y. Cat peripheral nerve regeneration across 50 mm gap repaired with a novel nerve guide composed of freeze-dried alginate gel. Neurosci Lett. 1999; 259(2): 75–78. PMID: 10025561

13. Ichihara S, Inada Y, Nakada A, Endo K, Azuma T, Nakai R, et al. Development of new nerve guide tube for repair of long nerve defects. Tissue Eng Part C Methods. 2009; 15(3): 387–402. https://doi.org/10.1089/ten.tec.2008.0508 PMID: 19226199

14. Sanders FK, Whitteridge D. Conduction velocity and myelin thickness in regenerating nerve fibres. J Physiol. 1946; 105(2): 152–174. PMID: 16991715

15. Rushton WA. A theory of the effects of fibre size in medullated nerve. J Physiol. 1951; 115(1): 101–122. PMID: 14889433

16. Lundborg G, Gelberman RH, Longo FM, Powell HC, Varon S. In vivo regeneration of cut nerves encased in silicone tubes: growth across a six-millimeter gap. J Neuropathol Exp Neurol. 1982; 41(4): 412–422. PMID: 7086464

17. Ide C, Tohyama K, Tajima K, Endoh K, Sano K, Tamura M, et al. Long acellular nerve transplants for allogenic grafting and the effects of basic fibroblast growth factor on the growth of regenerating axons in dogs: a preliminary report. Exp Neurol. 1998; 154(1): 99–112. https://doi.org/10.1006/exnr.1998.6921 PMID: 9875272

18. Millesi H, Meissl G, Berger A. The interfascicular nerve-grafting of the median and ulnar nerves. J Bone Joint Surg Am. 1972; 54(4): 727–750. PMID: 4560075

19. Millesi H. Nerve grafting. In: Terzis JK, editor. Microreconstruction of nerve injuries. Philadelphia: WB Saunders; 1987. pp. 223–237.

20. Dellon AL and Mackinnon SE. An alternative to the classical nerve graft for the management of the short nerve gap. Plast Reconstr Surg. 1988; 82(5): 849–856. PMID: 2845455

21. Evans GR. Challenges to nerve regeneration. Semin Surg Oncol. 2000; 19(3): 312–318. PMID: 11135488

22. Maquet V, Martin D, Malgrange B, Franzen R, Schoenen J, Moonen G, et al. Peripheral nerve regeneration using bioresorbable macroporous polylactide scaffolds. J Biomed Mater Res. 2000; 52(4); 639–651. PMID: 11033546

23. Martini R, Schachner M, Brushart TM. The L2/HNK-1 carbohydrate is preferentially expressed by previously motor axon-associated Schwann cells in reinnervated peripheral nerves. J Neurosci. 1994; 14(11 Pt 2): 7180–7191. PMID: 7525896

24. Zhang Y, Campbell G, Anderson PN, Martini R, Schachner M, Lieberman AR. Molecular basis of interactions between regenerating adult rat thalamic axons and Schwann cells in peripheral nerve grafts I. Neural cell adhesion molecules. J Comp Neurol. 1995; 361(2): 193–209. https://doi.org/10.1002/cne.903610202 PMID: 8543658

25. IJkema-Paassen J, Jansen K, Gramsbergen A, Meek MF. Transection of peripheral nerves, bridging strategies and effect evaluation. Biomaterials. 2004; 25(9): 1583–1592. PMID: 14697860

26. Rodríguez FJ, Verdú E, Ceballos D, Navarro X. Nerve guides seeded with autologous Schwann cells improve nerve regeneration. Exp Neurol. 2000; 161(2): 571–584. https://doi.org/10.1006/exnr.1999.7315 PMID: 10686077

27. de la Torre JC, Goldsmith HS. Increased blood flow enhances axon regeneration after spinal transection. Neurosci Lett. 1988; 94(3): 269–273. PMID: 2905029

28. Haapaniemi T, Nylander G, Kanje M, Dahlin L. Hyperbaric oxygen treatment enhances regeneration of the rat sciatic nerve. Exp Neurol. 1998; 149(2): 433–438. https://doi.org/10.1006/exnr.1997.6745 PMID: 9500969

29. Heumann R. Regulation of the synthesis of nerve growth factor. J Exp Biol. 1987; 132: 133–150. PMID: 3323396

30. Lindholm D, Heumann R, Meyer M, Thoenen H. Interleukin-1 regulates synthesis of nerve growth factor in non-neuronal cells of rat sciatic nerve. Nature. 1987; 330(6149): 658–659. https://doi.org/10.1038/330658a0 PMID: 3317065

31. Thoenen H, Bandtlow C, Heumann R, Lindholm D, Meyer M, Rohrer H. Nerve growth factor: cellular localization and regulation of synthesis. Cell Mol Neurobiol. 1988; 8(1): 35–40. PMID: 3042143

32. Fu SY, Gordon T. The cellular and molecular basis of peripheral nerve regeneration. Mol Neurobiol. 1997; 14(1–2): 67–116. https://doi.org/10.1007/BF02740621 PMID: 9170101

33. Kingham PJ, Terenghi G. Bioengineered nerve regeneration and muscle reinnervation. J Anat. 2006; 209(4): 511–526. https://doi.org/10.1111/j.1469-7580.2006.00623.x PMID: 17005023

34. De Luigi A, Terreni L, Sironi M, De Simoni MG. The sympathetic nervous system tonically inhibits peripheral interleukin-1beta and interleukin-6 induction by central lipopolysaccharide. Neuroscience. 1998; 83(4): 1245–1250. PMID: 9502262

35. Kim Y, Hamada N, Takahashi Y, Sasaguri K, Tsukinoki K, Onozuka M, et al. Cervical sympathectomy causes alveolar bone loss in an experimental rat model. J Periodontal Res. 2009; 44(6): 695–703. https://doi.org/10.1111/j.1600-0765.2008.01177.x PMID: 19453856

36. Alborch E, Gomez B, Dieguez G, Marin J, Lluch S. Cerebral blood flow and vascular reactivity after removal of the superior cervical sympathetic ganglion in the goat. Circ Res. 1977; 41(3): 278–282. PMID: 19161

37. Ghai A, Kaushik T, Kumar R, Wadhera S. Chemical ablation of stellate ganglion for head and neck cancer pain. Acta Anaesthesiol Belg. 2016; 67(1): 6–8. PMID: 27363209

38. Higa K, Hirata K, Hirota K, Nitahara K, Shono S. Retropharyngeal hematoma after stellate ganglion block: analysis of 27 patients reported in the literature. Anesthesiology 2006; 105(6): 1238–1245; discussion 5A-6A. PMID: 17122587

39. Wulf H, Maier C. [Complications and side effects of stellate ganglion blockade. Results of a questionnaire survey]. Anaesthesist. 1992; 41(3): 146–151. [Article in German]. PMID: 1570888

40. Narouze S. Ultrasound-guided stellate ganglion block: safety and efficacy. Curr Pain Headache Rep. 2014; 18(6): 424. https://doi.org/10.1007/s11916-014-0424-5 PMID: 24760493

41. Liao CD, Tsauo JY, Liou TH, Chen HC, Rau CL. Efficacy of noninvasive stellate ganglion blockade performed using physical agent modalities in patients with sympathetic hyperactivity-associated disorders:

a systematic review and meta-analysis. PLoS One. 2016; 11(12): e0167476. https://doi.org/10.1371/journal.pone.0167476 PMID: 27911934

42. Liao CD, Rau CL, Liou TH, Tsauo JY, Lin LF. Effects of linearly polarized near-infrared irradiation near the stellate ganglion region on pain and heart rate variability in patients with neuropathic pain. Pain Med. 2017; 18(3): 488–503. https://doi.org/10.1093/pm/pnw145 PMID: 27452896